Acta Crystallographica Section D
Biological Crystallography
ISSN 0907-4449

Structure of *Escherichia coli* BamD and its functional implications in outer membrane protein assembly

Cheng Dong,[a,b] Hai-Feng Hou,[a] Xue Yang,[b] Yue-Quan Shen[b] and Yu-Hui Dong[a]*

[a]Beijing Synchrotron Radiation Facility, Institute of High Energy Physics, Chinese Academy of Sciences, Beijing 100049, People's Republic of China, and [b]Tianjin Key Laboratory of Protein Science, College of Life Science, Nankai University, Tianjin 300071, People's Republic of China

Correspondence e-mail: dongyh@ihep.ac.cn

Received 4 August 2011
Accepted 28 November 2011

PDB Reference: BamD, 3q5m.

The outer membrane protein complex (BAM complex) plays an important role in outer membrane protein (OMP) assembly in *Escherichia coli*. The BAM complex includes the integral β-barrel protein BamA as well as four lipoproteins: BamB, BamC, BamD and BamE. One of these lipoproteins, BamD, is essential for the survival of *Escherichia coli*. The structure of BamD at 2.6 Å resolution shows that this lipoprotein is composed of ten α-helices that form five tetratricopeptide-repeat (TPR) motifs. The arrangement of the BamD motifs is similar to that in the periplasmic part of BamA. One of the ten α-helices, α10, which has been shown to be important for the assembly of the BAM complex, is located in the very C-terminal region of BamD. A deep groove between TPR domains 4 and 5 is also observed. This groove, as well as the surface around α10, may provide binding sites for other components of the BAM complex. The C-terminal region of BamD serves as a platform for interactions with other components of the BAM complex. The N-terminal region shares structural similarity to other proteins whose functions are related to assistance in or regulation of secretion. Therefore, this region is likely to play an important role in the insertion of other outer membrane proteins.

1. Introduction

The assembly of β-barrel proteins into the membrane is a fundamental process that is essential in Gram-negative bacteria, mitochondria and plastids (Voulhoux *et al.*, 2003). In *Escherichia coli*, the outer membrane protein complex (BAM complex) is essential for outer membrane protein assembly (Werner & Misra, 2005; Doerrler & Raetz, 2005). Recent studies have shown that the BAM complex includes the integral β-barrel protein BamA (YaeT) and the lipoproteins BamB (YfgL), BamC (NlpB), BamD (YfiO) and BamE (SmpA) (Wu *et al.*, 2005; Sklar *et al.*, 2007).

The component BamA itself is also an outer membrane protein. Deletion of this component causes lethal damage to *E. coli* cells (Doerrler & Raetz, 2005). BamA consists of two regions: an N-terminal region containing five polypeptide transport-associated (POTRA) domains and a C-terminal β-barrel domain (Sánchez-Pulido *et al.*, 2003). It is clear that BamA acts as the core of the BAM complex and interacts stably with the associated BamC, BamD and BamE components *via* the POTRA domains (Robert *et al.*, 2006; Kim *et al.*, 2007).

The structures of the five POTRA domains of BamA have recently been characterized by X-ray crystallography, NMR and small-angle X-ray scattering (SAXS) (Kim *et al.*, 2007; Gatzeva-Topalova *et al.*, 2008, 2010). The five POTRA domains have similar folds and are composed of three-

stranded β-sheets and a pair of antiparallel helices. The arrangement of the four domains from POTRA1 to POTRA4 can be characterized as a fish-hook-like shape (Kim *et al.*, 2007), while another structure revealed conformational flexibility around a hinge point between the POTRA2 and the POTRA3 domains (Gatzeva-Topalova *et al.*, 2008). Crystallographic and NMR solution structures of the POTRA4–5 domains also revealed conformational flexibility between POTRA4 and POTRA5 (Gatzeva-Topalova *et al.*, 2010). According to these results, the region composed of POTRA1 and POTRA2 and the region composed of POTRA3 and POTRA4 are relatively rigid, while the conformations of POTRA2–3 and POTRA4–5 are flexible.

The functions of the POTRA domains have also been studied systematically. A POTRA deletion mutant assay suggested that POTRA1 has no effect on the interactions of BamA with BamB, BamC, BamD and BamE. However, only POTRA2, POTRA3 and POTRA4 are required to mediate the interaction with BamB, whereas POTRA5 is crucial for the interaction with all of the lipoproteins in the BAM complex (Kim *et al.*, 2007). The structural flexibility within the POTRA domains reveals the details of their interactions with the components within the BAM complex and the insertion mechanism for the outer membrane proteins.

The BAM complex has recently been successfully assembled *in vitro* (Hagan *et al.*, 2010) and the interactions as well as the importance of the components have been intensively studied. BamB and BamD make direct contacts with BamA, while BamC requires the C-terminus of BamD for interaction with BamA (Malinverni *et al.*, 2006). BamE interacts directly with BamA, BamC and BamD, but not with BamB (Sklar *et al.*, 2007).

In the BAM complex, BamD is a core component for OMP assembly, as is BamA. Both of these proteins are essential for cell viability and OMP biogenesis; even deletion of the C-terminal part of BamD decreases the density of the outer membrane, disturbs the assembly of OMPs and elevates the level of DegP. Therefore, BamD plays a critical role in the BamA-mediated OMP folding pathway, whereas null mutants of BamB, BamC and BamE are viable, albeit with defects in OMP assembly (Wu *et al.*, 2005; Sklar *et al.*, 2007; Malinverni *et al.*, 2006). Furthermore, the interactions between BamC/BamE and BamA are mediated by BamD (Sklar *et al.*, 2007; Malinverni *et al.*, 2006). Therefore, we anticipate that the structure of BamD will reveal details of the interactions between components in the BAM complex, as well as the possible role of BamD in the folding and insertion of the outer membrane proteins.

2. Materials and methods

2.1. Cloning and expression

The gene encoding BamD (amino acids 23–245) was amplified from genomic *E. coli* DNA *via* PCR using sense (5′-GGCCATATGTCAAAGGAAGAAGTACCTGA) and antisense (5′-ACGGAATTCTTATGTATTGCTGCTGTTTGCGGCGAT) primers which contain *Nde*I and *Eco*RI restriction sites, respectively. The purified PCR products were digested with *Nde*I and *Eco*RI and then ligated into a modified pET28a expression vector (Novagen, USA) in which a PreScission Protease site replaced the thrombin protease site and six additional His residues were added at the N-terminus. The recombinant plasmid was transformed into *E. coli* BL21 (DE3) (Invitrogen) competent cells for expression. Overexpression of BamD was induced using 0.1 m*M* isopropyl β-D-1-thiogalactopyranoside (IPTG) when the cell density reached an OD_{600} of 0.6 in LB medium with 50 µg ml^{-1} kanamycin at 310 K. After further incubation overnight at 298 K, the cells were harvested by centrifugation at 5000 rev min^{-1} for 15 min.

2.2. Protein purification

The cell pellets were resuspended in lysis buffer (20 m*M* Tris–HCl, 200 m*M* NaCl pH 8.5) supplemented with 0.1 m*M* phenylmethylsulfonyl fluoride (PMSF) and lysed on ice by sonication. The crude cell extract was clarified by centrifugation at 18 000 rev min^{-1} for 60 min and the supernatant was passed through an Ni–NTA column (GE Healthcare, USA) pre-equilibrated with lysis buffer. The impurities were washed out with lysis buffer containing 50 m*M* imidazole and the target protein BamD was eluted with 300 m*M* imidazole. The eluate was treated overnight with PreScission Protease at 277 K to remove the N-terminal His_6 tag, and the imidazole was removed by dialysis. As a result, four additional residues (Gly-Pro-His-Met) were left at the N-terminus of BamD. The mixture was reloaded onto an Ni–NTA column and the flowthrough was concentrated. The flowthrough was then passed through a Superdex 200 column (GE Healthcare, USA) using a buffer consisting of 20 m*M* Tris–HCl, 100 m*M* NaCl pH 8.5. Based on the results of gel-filtration chromatography, it was deduced that BamD exists as a monomer in solution. The purity of the protein was analyzed by SDS–PAGE at each step and the purified protein was concentrated to $\sim$20 mg ml^{-1} and subjected to crystallization trials.

2.3. Crystallization

Eight different screening kits from Hampton Research (Crystal Screen, Crystal Screen 2, Index, PEGRx, PEG/Ion, Natrix, SaltRx and Grid Screen PEG/LiCl) were employed to screen for crystals of BamD. A crystal of native BamD was grown after two weeks *via* the sitting-drop vapour-diffusion technique using 20%(*w*/*v*) PEG 3350 and 0.20 *M* potassium iodide (PEG/Ion kit) as the reservoir buffer. The sitting-drop crystallization trials were performed at 277 K by mixing 1 µl protein solution with 1 µl reservoir solution. Further experiments were performed to optimize the preliminary conditions, including the salt concentration and precipitant concentration. The crystal of BamD used for data collection was obtained under optimized conditions consisting of 27%(*w*/*v*) PEG 3350 and 0.28 *M* potassium iodide. A selenomethionine (SeMet) derivative was purified as described above. The purified SeMet protein was concentrated to $\sim$20 mg ml^{-1} for crystallization, but it was difficult to obtain high-quality crystals of the SeMet derivative even after intensive trials and optimization. Finally,

Table 1
Data-collection and refinement statistics for BamD.

Values in parentheses are for the highest resolution shell.

Space group	$P4_122$
Unit-cell parameters (Å)	$a = b = 106.55$, $c = 65.07$
Wavelength (Å)	0.9791
Resolution range (Å)	30–2.60 (2.69–2.60)
No. of unique reflections	11644
Multiplicity	23.3 (10.4)
R_{merge}† (%)	13.3 (64.3)
$\langle I/\sigma(I)\rangle$	41.1 (2.8)
Completeness (%)	99.9 (99.9)
FOM	0.643
Refinement	
R_{cryst}‡ (%)	21.6
R_{free}§ (%)	26.1
R.m.s.d.$_{bond}$ (Å)	0.009
R.m.s.d.$_{angle}$ (°)	1.2
No. of protein atoms	1694
No. of ligand atoms	7
No. of solvent atoms	22
Ramachandran plot, residues in (%)	
Most favoured region	88.8
Additionally allowed region	10.6
Generously allowed region	0.5
Disallowed region	0
Average B factor of protein (Å^2)	54.8

† $R_{merge} = \sum_{hkl}\sum_i |I_i(hkl) - \langle I(hkl)\rangle| / \sum_{hkl}\sum_i I_i(hkl)$. ‡ $R_{cryst} = \sum_{hkl} ||F_{obs}| - |F_{calc}|| / \sum_{hkl} |F_{obs}|$. § R_{free} is calculated in the same way as R_{cryst} but from a test set containing 5% of the data, which were excluded from refinement.

crystals of the SeMet derivative were grown using a streak and microseeding assay (Bergfors, 2003). The seeds for crystallization were obtained from native crystals of BamD.

2.4. Data collection

Prior to data collection, the crystals were cooled in a cryoprotectant consisting of the reservoir solution supplemented with 25% glycol. A single anomalous dispersion data set was collected at the peak wavelength for Se on the BL17U beamline at the Shanghai Synchrotron Radiation Facility (SSRF). Diffraction experiments were conducted at 100 K and images were recorded on a Rayonix MX-225 CCD detector. The data were processed using the *HKL*-2000 software (Otwinowski & Minor, 1997). The BamD crystal belonged to space group $P4_122$ and diffracted to 2.6 Å resolution, with unit-cell parameters $a = b = 106.55, c = 65.07$ Å, $\alpha = \beta = \gamma = 90.00°$. The crystals contained one molecule per asymmetric unit.

2.5. Structure determination

The program *HKL2MAP* (Pape & Schneider, 2004) was used to search for the seven Se sites and initial phases were then calculated using the *PHENIX* software (Adams *et al.*, 2010) Model building and refinement were performed using *Coot* (Emsley & Cowtan, 2004) and *PHENIX*. After the initial alanine model had been built, iterative refinement was performed to assign all of the side chains. After several refinement cycles using the refinement programs *PHENIX* and *Coot*, the orientations of the amino-acid side chains and bound water molecules were modelled *via* $2F_o - F_c$ and $F_o - F_c$ difference Fourier maps. The final structure had an R_{cryst} value of 21.6% and an R_{free} value of 26.1%. A Ramachandran plot created by the program *PROCHECK* (Laskowski *et al.*, 1993) showed that 88.8% of the residues were in the most favoured regions, 10.6% of the residues were in additional allowed regions, 0.5% of the residues were in generously allowed

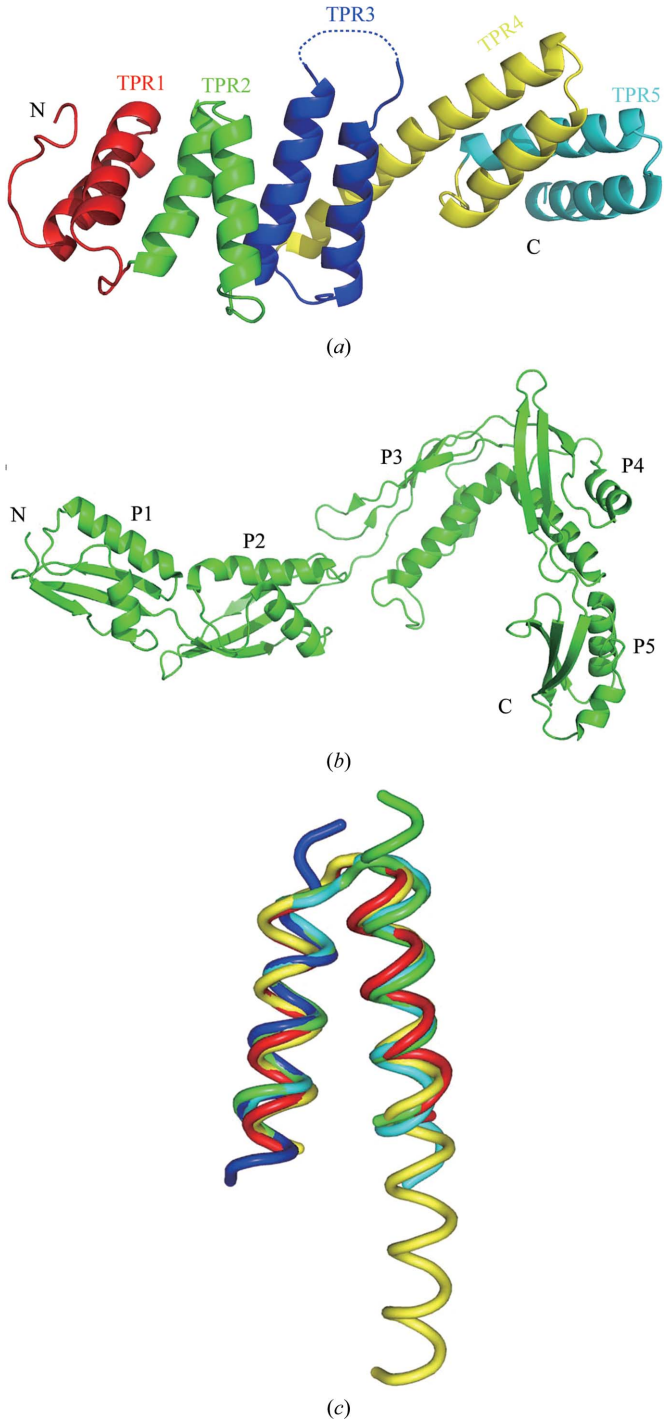

Figure 1
The overall structures of BamD and BamA. (*a*) The structure of BamD is composed of ten helices and the loops that connect them. The ten helices can be divided into five TPR domains. (*b*) The overall structure of POTRA1–5 (P1–5) of BamA and the overall domain arrangement are quite similar to those of BamD. (*c*) Superposition of the five TPR domains in BamD. TPR1, red; TPR2, green; TPR3, blue; TPR4, yellow; TPR5, cyan. The five TPR domains of BamD are quite similar, although α7 is much longer in TPR4

regions and none of the residues were in disallowed regions. Detailed data-collection and refinement statistics are given in Table 1. Structure figures were generated using the *PyMOL* software (DeLano, 2002).

3. Results and discussion

3.1. The overall structure of BamD

The structure of *E. coli* BamD was solved using the single-wavelength anomalous dispersion (SAD) method at 2.6 Å resolution. The final model of *E. coli* BamD contained residues 23–243 of BamD, with the exception of residues 122–134, which were not traceable in the electron-density map owing to their flexibility. The missing residues form a loop connecting two α-helices and separate the entire BamD molecule into two parts (Fig. 1*a*).

The structure of BamD is composed of ten α-helices and the loops connecting them; no β-sheets were found. The ten α-helices can also be divided into five tetratricopeptide-repeat (TPR) motifs. Each TPR domain includes two neighbouring α-helices and a connecting loop, which is a typical helix–loop–helix motif. The five successive TPR motifs rotate in a right-handed direction. The overall structure of BamD is shown in Fig. 1(*a*).

The lengths of nine of the ten α-helices in BamD are approximately the same, with each helix containing 13–17 residues. The exception is α7 in TPR domain 4: this long helix is composed of 29 residues. Superposition of the five TPR domains shows that TPR domains 1, 2, 3 and 5 are quite similar, while TPR domain 4 is unique owing to the long α-helix (Fig. 1*c*). The r.m.s.d. values between the TPR domains of BamD are listed in Table 2.

The overall domain arrangement of BamD is quite similar to that of the periplasmic region of BamA (Fig. 1*b*). The periplasmic portion of BamA consists of five POTRA domains, while BamD is made up of five TPR domains, and the respective arrangements of these domains are similar in the two molecules. Furthermore, the orientations of the five

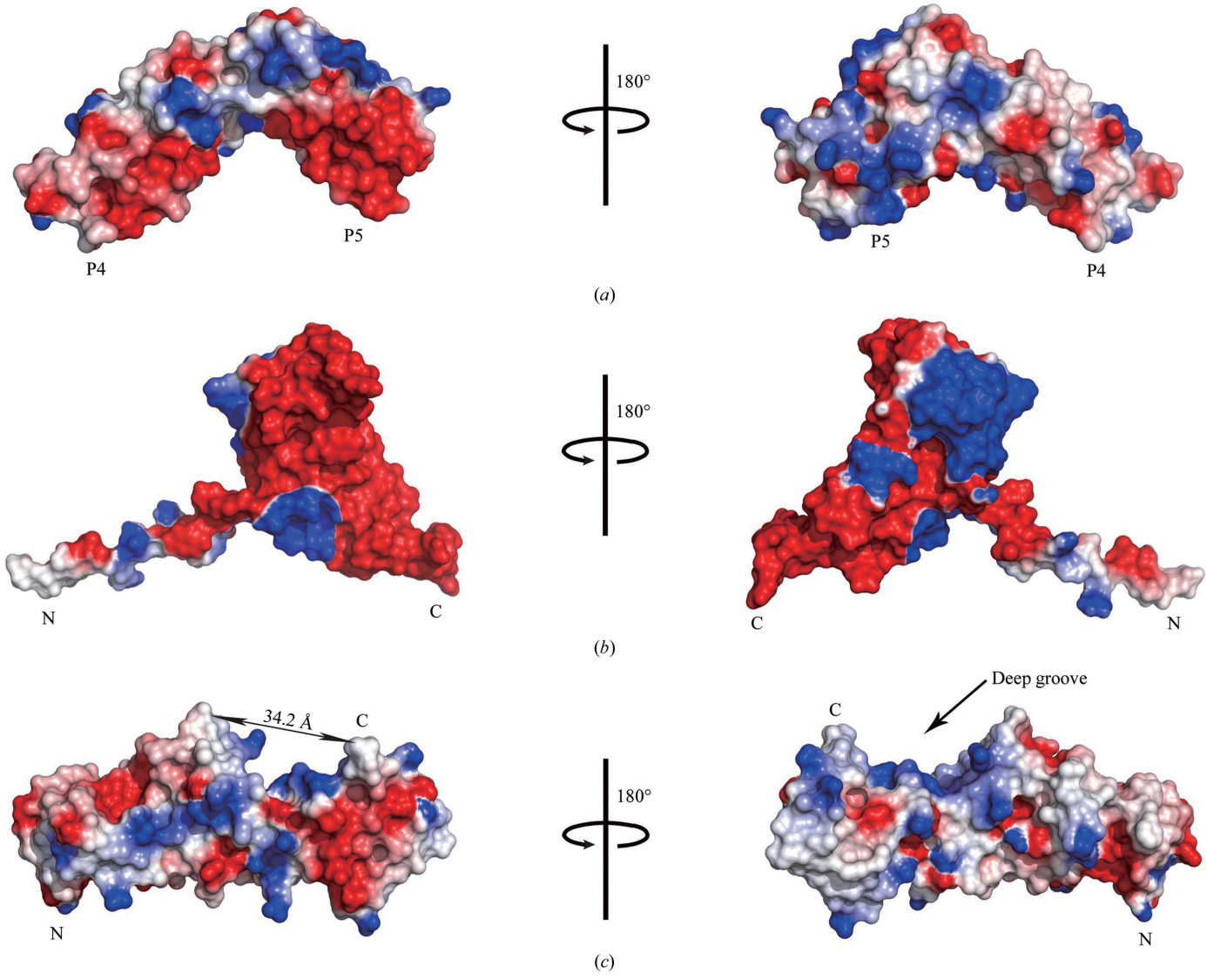

Figure 2
The surface-charge distributions of POTRA4–5 (*a*), BamE (*b*) and BamD (*c*). A deep groove is located in the C-terminal region of BamD.

Table 2
R.m.s.d. between TPR domains of BamD.

	R.m.s.d. (Å)	Aligned residues
TPR1–TPR2	0.70	30
TPR1–TPR3	0.57	30
TPR1–TPR4	0.56	29
TPR1–TPR5	0.69	30
TPR2–TPR3	0.76	32
TPR2–TPR4	0.40	15
TPR2–TPR5	0.77	31
TPR3–TPR4	0.66	30
TPR3–TPR5	0.78	31
TPR4–TPR5	0.96	32

domains in both molecules are variable and essential for their function. The similarity in structure between BamD and BamA suggests the possibility that BamD may function as a scaffold to mediate protein–protein interactions. These interactions include not only the interactions between the components of the BAM complex but also those with the target OMPs that are inserted into the outer membrane.

3.2. The implications for interaction surfaces and the possible function of the C-terminal region

The structure of BamD we obtained exhibits a deep groove, which lies in the C-terminal region and is surrounded by TPR domains 4 and 5 (Fig. 2*c*). The width of this groove is 34.2 Å. The TPR motif is a typical protein–protein interaction module that also provides several grooves for ligand binding (Scheufler *et al.*, 2000).

It has been reported that POTRA5 in BamA is necessary for the interaction of BamA with BamD (Kim *et al.*, 2007). BamC, BamD and BamE interact with each other, and the C-terminus of BamD (residues 226–245), corresponding to helix α10 in our structure, is required to maintain a stable interaction between BamA, BamC and BamE (Wu *et al.*, 2005; Robert *et al.*, 2006). Therefore, helix α10 of BamD plays an essential role in the interactions between BamA, BamC and BamE.

To analyze the potential interface in BamD that is involved in BAM complex interactions, we examined the electrostatic properties of the POTRA4–5 region of BamA, BamD and BamE (Fig. 2). The results show that the many of the negatively charged residues in POTRA5 are clustered on one side of the molecule and positively charged residues accumulate on the opposite side. The surface of BamE depicts a large area of negative charge and the residues which are critical for binding to BamD, *i.e.* Arg29, Ile32, Tyr37, Leu38, Thr61, Leu63, Phe68, Asn71, Thr72, Trp73, Arg78, Thr92 and Phe95 (Knowles *et al.*, 2011), are exposed in the negatively charged region (Fig. 3*a*). The C-terminal region of BamD appears to comprise a largely negatively charged region. However, the charge distribution around α10 is amphoteric (Fig. 3*b*), *i.e.* the positively charged residues Lys233 and Lys236 of α10 are located on one side, while the other side is formed by the negatively charged residues Glu232 of α10 and Glu219 of the adjacent α9. This observation suggests that helix α10 may be clamped between the positively charged region of POTRA5 and the negatively charged region of BamE.

In summary, we suggest that the C-terminal region of BamD, especially helix α10, serves as the link between BamA, BamC and BamE. The deep groove, as well as the surface around α10, provides the binding pockets. Deletion of helix α10 leads to loss of BamC and BamE from the BAM complex, but the functional components, *i.e.* the N-terminal region of BamD and BamA, are still located on the membrane and therefore the cells are still viable. In such cases, owing to the loss of the interaction between BamA and BamD, the efficiency of the folding and insertion of OMPs should be reduced and therefore the steady levels of OMPs are lower and the level of DegP increases, as observed in experiments by other groups (Malinverni *et al.*, 2006).

3.3. The conserved amino acids and the possible function of the N-terminal region

Several studies have shown that cells are viable despite the fact that the C-terminus of BamD has inserted transposons (Gatzeva-Topalova *et al.*, 2008; Kim *et al.*, 2007). Therefore, the essential portion for the function of BamD is the N-terminal region rather than the C-terminal region.

The sequence alignment of *E. coli* BamD and its homologues from other Gram-negative bacterial species revealed a number of conserved amino acids, with a particularly high

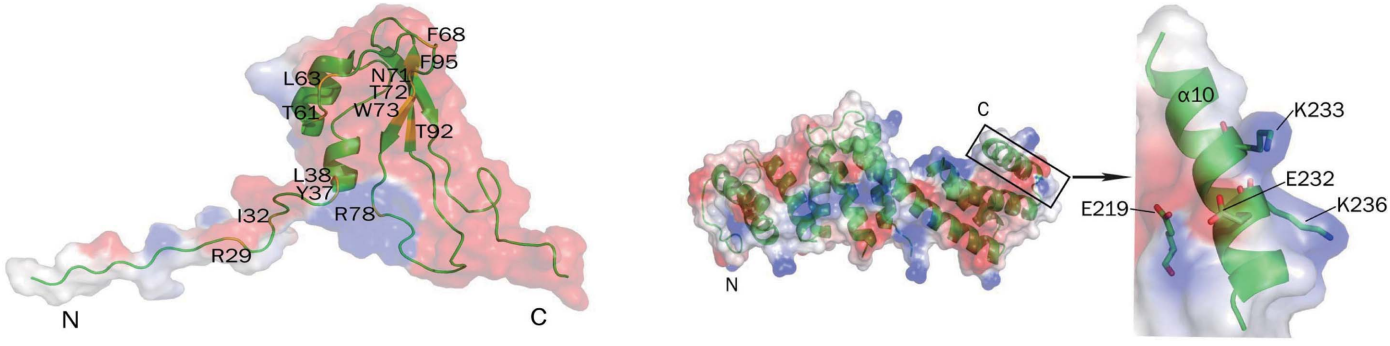

Figure 3
(*a*) The residues that are important for binding to BamD are located in the negatively charged surface of BamE. (*b*) The C-terminal region of BamD contains a negatively charged region, while the charge distribution around α10 is amphoteric.

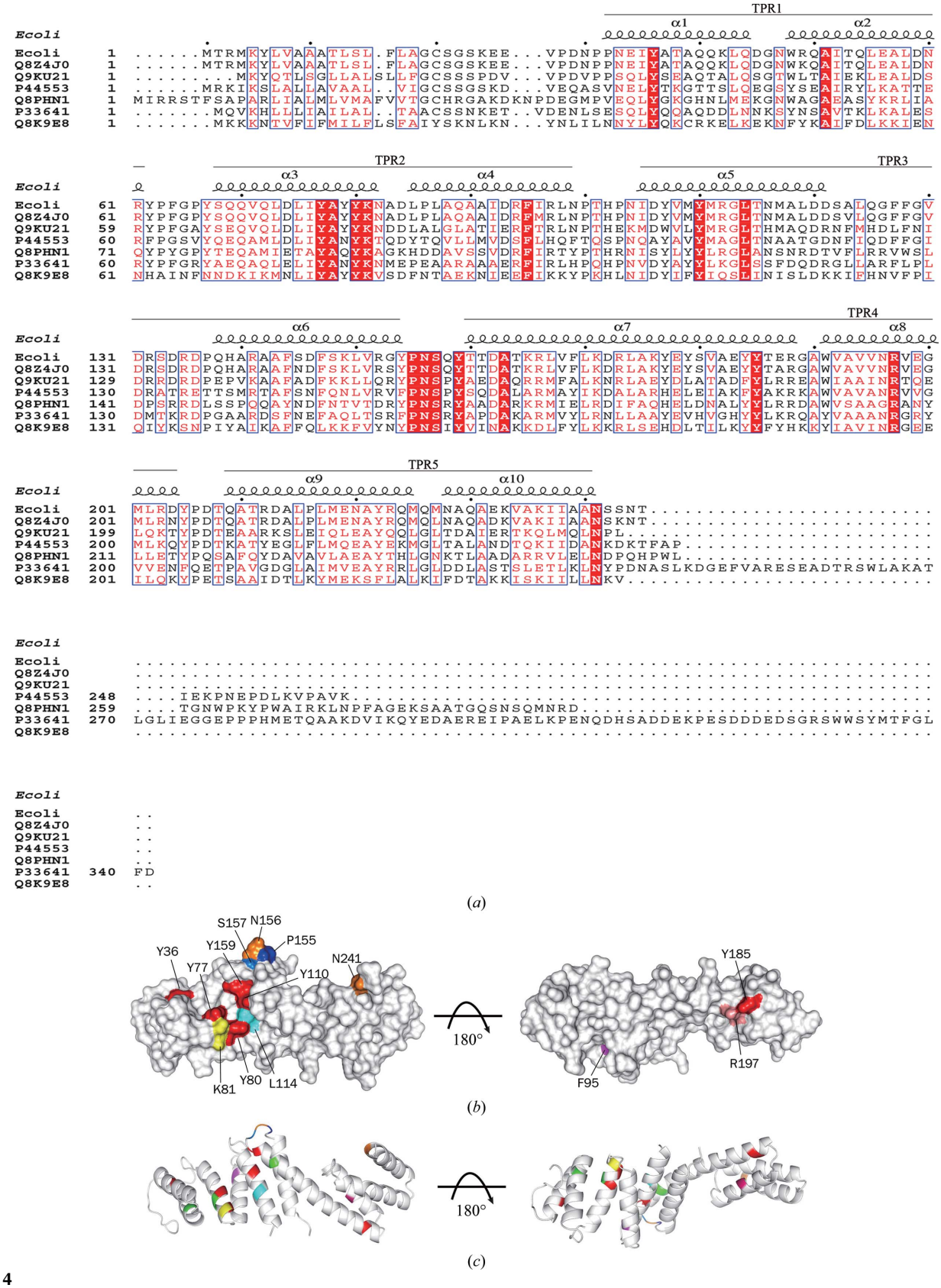

Figure 4
Conserved amino acids within BamD homologues in Gram-negative bacteria. (*a*) Sequence alignment of BamD and its homologues in other Gram-negative bacterial species. Absolutely conserved residues are shown on a red background, similar residues in red and stretches of residues that are similar across the group of sequences in blue boxes. The protein sequences were obtained from the UniProtKB database: *Salmonella typhi*, Q8Z4J0; *Vibrio cholera*, Q9KU21; *Haemophilus influenza*, P44553; *Xanthomonas axonopodis* pv. *citri*, Q8PHN1; *Pseudomonas aeruginosa*, P33641; *Buchnera aphidicola* subsp. *Schizaphis graminum*, Q8K9E8. (*b*, *c*) Mapping of the conserved residues onto the surface representation (*b*) and ribbon representation (*c*).

conservation of tyrosines (Fig. 4*a*). The majority of the conserved residues are exposed on the surface of BamD (Figs. 4*b* and 4*c*), except for the conserved alanines Ala51, Ala78 and Ala163. Interestingly, the loop between the TPR3 and TPR4 domains consists almost entirely of conserved residues (Pro155, Asn156, Ser157 and Tyr159), which are exposed at the top of the groove. The residues that are located in the missing loop in the electron-density map (between α5 and α6) are relatively nonconserved. The fact that the conserved residues of BamD are mainly located on the surface in the N-terminal region of BamD is consistent with its requirement for the function of BamD (Kim *et al.*, 2007; Knowles *et al.*, 2009) and implies that the achievement of said function relies on the interactions between BamD and other proteins.

We used the *DALI* server (Holm *et al.*, 2008) to search for structural homologues of BamD and several proteins were identified that have similar structures to BamD. These proteins included YbgF from *Xanthomonas campestris* (PDB entry 2xev; *Z* score 17.2, r.m.s.d. 1.6 Å; Krachler *et al.*, 2010), IpgC from *Shigella flexneri* (PDB entry 3gz1; *Z* score 15.6, r.m.s.d. 2.2 Å; Lunelli *et al.*, 2009), SycD from *Yersinia enterocolitica* (PDB entry 2vgx; *Z* score 15.0, r.m.s.d. 2.5 Å; Büttner *et al.*, 2008), the TPR domain of the human small glutamine-rich tetratricopeptide-repeat protein (SGT; PDB entry 2vyi; *Z* score 13.2, r.m.s.d. 2.3 Å; Dutta & Tan, 2008), the TPR2A domain of HOP (PDB entry 1elr; *Z* score 13.9, r.m.s.d. 2.7 Å; Scheufler *et al.*, 2000), PcrH from *Pseudomonas aeruginosa* (PDB entry 2xcc; *Z* score 14.8, r.m.s.d. 2.5 Å; Job *et al.*, 2010) and a structure designed from an idealized TPR motif (PDB entry 1na0; *Z* score 14.8, r.m.s.d. 2.0 Å; Main *et al.*, 2003). The structural alignment is shown in Fig. 5. All of these proteins share a significant degree of similarity with the N-terminal region of BamD and might help to provide some clues to the function of this region of BamD. In the type III secretion system, IpgC, SycD and PcrH have an effect on secretion, biosynthesis and transport processes, respectively, by acting as chaperones (Barta *et al.*, 2010; Büttner *et al.*, 2008; Job *et al.*, 2010), the SGT protein belongs to a family of co-chaperones and inhibits viral particle release (Dutta & Tan, 2008) and the Hop protein participates in the ordered assembly of Hsp70–Hsp90 multichaperone complexes (Scheufler *et al.*, 2000).

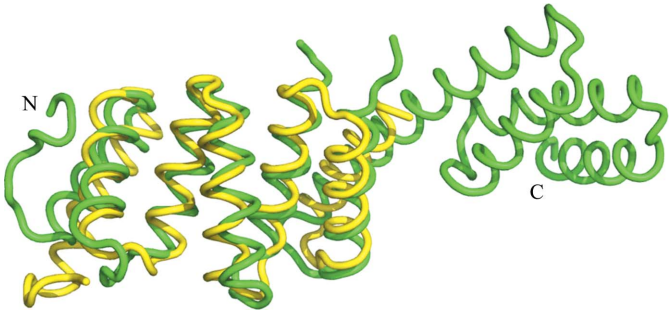

Figure 5
Superposition of the N-terminal region of BamD and structural homologues. For clarity, only the result of superposition of the N-terminal region of BamD (green) and IpgC from *Shigella flexneri* (PDB entry 3gz1, yellow) is shown.

It can be concluded that the TPR domain is a protein-interaction platform, but its interaction partners are diverse. Extensive evidence indicates that TPR motifs are functionally important in chaperones, the cell cycle, transcription and protein-transport complexes. The diversity of interaction partners may be necessary for the recruitment of different proteins and adaptation to specific functions. The similarity between the N-terminal region of BamD and the structures mentioned above implies that the N-terminal region of BamD might also interact with various kinds of proteins as a chaperone to assist in the folding and insertion of OMPs into the outer membrane.

References

Adams, P. D. *et al.* (2010). *Acta Cryst.* D**66**, 213–221.
Barta, M. L., Zhang, L., Picking, W. L. & Geisbrecht, B. V. (2010). *BMC Struct. Biol.* **10**, 21.
Bergfors, T. (2003). *J. Struct. Biol.* **142**, 66–76.
Büttner, C. R., Sorg, I., Cornelis, G. R., Heinz, D. W. & Niemann, H. H. (2008). *J. Mol. Biol.* **375**, 997–1012.
DeLano, W. L. (2002). *PyMOL*. http://www.pymol.org.
Doerrler, W. T. & Raetz, C. R. (2005). *J. Biol. Chem.* **280**, 27679–27687.
Dutta, S. & Tan, Y.-J. (2008). *Biochemistry*, **47**, 10123–10131.
Emsley, P. & Cowtan, K. (2004). *Acta Cryst.* D**60**, 2126–2132.
Gatzeva-Topalova, P. Z., Walton, T. A. & Sousa, M. C. (2008). *Structure*, **16**, 1873–1881.
Gatzeva-Topalova, P. Z., Warner, L. R., Pardi, A. & Sousa, M. C. (2010). *Structure*, **18**, 1492–1501.
Hagan, C. L., Kim, S. & Kahne, D. (2010). *Science*, **328**, 890–892.
Holm, L., Kääriäinen, S., Rosenström, P. & Schenkel, A. (2008). *Bioinformatics*, **24**, 2780–2781.
Job, V., Matteï, P. J., Lemaire, D., Attree, I. & Dessen, A. (2010). *J. Biol. Chem.* **285**, 23224–23232.
Kim, S., Malinverni, J. C., Sliz, P., Silhavy, T. J., Harrison, S. C. & Kahne, D. (2007). *Science*, **317**, 961–964.
Knowles, T. J. *et al.* (2011). *EMBO Rep.* **12**, 123–128.
Knowles, T. J., Scott-Tucker, A., Overduin, M. & Henderson, I. R. (2009). *Nature Rev. Microbiol.* **7**, 206–214.
Krachler, A. M., Sharma, A., Cauldwell, A., Papadakos, G. & Kleanthous, C. (2010). *J. Mol. Biol.* **403**, 270–285.
Laskowski, R. A., MacArthur, M. W., Moss, D. S. & Thornton, J. M. (1993). *J. Appl. Cryst.* **26**, 283–291.
Lunelli, M., Lokareddy, R. K., Zychlinsky, A. & Kolbe, M. (2009). *Proc. Natl Acad. Sci. USA*, **106**, 9661–9666.
Main, E., Xiong, Y., Cocco, M., D'Andrea, L. & Regan, L. (2003). *Structure*, **11**, 497–508.
Malinverni, J. C., Werner, J., Kim, S., Sklar, J. G., Kahne, D., Misra, R. & Silhavy, T. J. (2006). *Mol. Microbiol.* **61**, 151–164.
Otwinowski, Z. & Minor, W. (1997). *Methods Enzymol.* **276**, 307–326.
Pape, T. & Schneider, T. R. (2004). *J. Appl. Cryst.* **37**, 843–844.
Robert, V., Volokhina, E. B., Senf, F., Bos, M. P., Van Gelder, P. & Tommassen, J. (2006). *PLoS Biol.* **4**, e377.
Sánchez-Pulido, L., Devos, D., Genevrois, S., Vicente, M. & Valencia, A. (2003). *Trends Biochem. Sci.* **28**, 523–526.
Scheufler, C., Brinker, A., Bourenkov, G., Pegoraro, S., Moroder, L., Bartunik, H., Hartl, F. U. & Moarefi, I. (2000). *Cell*, **101**, 199–210.
Sklar, J. G., Wu, T., Gronenberg, L. S., Malinverni, J. C., Kahne, D. & Silhavy, T. J. (2007). *Proc. Natl Acad. Sci. USA*, **104**, 6400–6405.
Voulhoux, R., Bos, M. P., Geurtsen, J., Mols, M. & Tommassen, J. (2003). *Science*, **299**, 262–265.
Werner, J. & Misra, R. (2005). *Mol. Microbiol.* **57**, 1450–1459.
Wu, T., Malinverni, J., Ruiz, N., Kim, S., Silhavy, T. J. & Kahne, D. (2005). *Cell*, **121**, 235–245.